# EG31: Underwater ERT method to image Karst cave distribution below the river water

*Daopu Wang[1]*, Haibin Chai[2], Dikun Yang[1], Banglai Lv[2]*
*1. The Department of Earth and Space Sciences, Southern University of Science and Technology, Shenzhen, China.*
*2. CCCC-FHDI Engineering Co., Ltd.*

**Summary**

Electrical resistivity tomography (ERT) was employed to locate potential karst cave areas beneath rivers. This study set up six 700-meter-long ERT survey lines across the East River. Using the specially designed 200-meter underwater cable with 5-meter electrode spacing, a pole-dipole electrode configuration was utilized to conduct observations of the underground structures. The inverted resistivity profiles revealed high-resistance anomalies in the surface layer and bedrock which were interpreted to be gravel, pebble, and limestone. Meanwhile, they delineated the spatial distribution of low-resistance anomalies such as sandstone and conglomerate. Deploying electrodes in water to observe underground resistivity structures is highly challenging, nevertheless it will provide guidance significant for subsequent underwater geological structure imaging.

**Introduction**

Areas where limestone is developed, are prone to underground water erosion and cave formation which give rise to geological structures such as fractures. Underground caves can cause ground collapse and uneven subsidence, seriously threatening the safety of people's lives, property, and engineering construction. Using geophysical methods to depict the spatial and morphological characteristics and distribution of subsurface caves can provide guidance for construction design and avoiding risk area. Electrical resistivity tomography (ERT) is based on direct current resistance. By injecting current into the ground and observing the distribution of potential differences between the surface electrodes, the distribution of underground resistivity structures and hence the geological structures can be obtained. In field observation, multiple electrodes are arranged at the same time. The positions of the current and potential electrodes are changed automatically by the acquisition device. The use of multi-channel measurement allows multiple observations of underground targets in a short time, which greatly improves the accuracy of exploration and construction efficiency. As ERT can produce high-resolution images of formations at shallow depths, it has been widely used in archaeological prospecting, detection of groundwater contamination and seawater intrusion, soil moisture analysis, and hydrogeological research [1,2,3,4,5].

In this study, we use the ERT method to collect electrical data from a small hydropower dam to be built on the Dongjiang River in Huizhou City. The existing borehole data help identify the potential areas of karst caves. The observation target is covered by river water with rapid flow, bringing great difficulties to dam construction. In the work area, we lay out 6 ERT lines of 700 meters (Fig.1). Using a specially made underwater cable of 200m with the electrode spacing of 5m, data are collected using pole-dipole electrode configuration. After the first round of observation, we move the cable forward along the survey line with half the length overlapping with the last observation. The process is repeated until the entire survey line was covered. From the field data, we use the open-source program SimPEG [6] to obtain the two-dimensional inversion of the underground electrical anomaly distribution and propose the potential locations of karst caves.

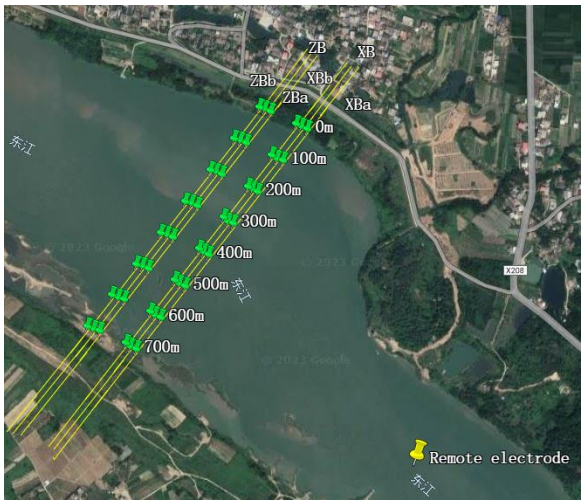


Figure 1: The map of the study area with the ERT survey profiles. XB refers to the survey line covering the lower half of the dam. XBa and XBb are survey lines 15 m downstream and upstream away of XB, respectively. ZB is the survey line covering the middle part of the dam. ZBa and ZBb are survey lines 15 m upstream and downstream away of ZB, respectively. The remote electrode is at the lower right corner of the figure.

**Method**

The research area consists of the middle and lower parts of the dam. According to the geology and drilling results, a 10

m layer of poorly sorted sand, gravel, and pebbles sits right below the water surface. Under this layer, it is the layer of sandstone, shale, phyllite, and weathered limestone with the thickness varying from 10–40 m. The bedrock is primarily limestone. According to borehole surveys in the working area, the shallowest cave is about 25 m below the water surface. Meanwhile, river water covers the target with a depth range of 0. 5–7 m.

It is very important to design appropriate survey lines and electrode arrangements due to the complexity of the construction environment. We implement a set of underwater cable with 40 electrodes and electrode spacing of 5m, to cover the effective length of 195 m. In the two areas, we lay out three survey lines crossing the Dongjiang River of 700 meter long with the line spacing of 15 m and an effective detection depth of 60m. Different electrode arrangements will result in different the apparent resistivity measurement [7]. The specific electrical array is selected based on the geological conditions of the working area, the resolution of the anomaly body, and the sensitivity to noise. Before the formal observation, we choose dipole-dipole and pole-dipole electrode arrays, both with good signal-to-noise ratios. The former has the advantage of horizontal resolution, while the latter can penetrate greater depths with the transmitted current [8].

Pilot surveys are conducted in the lower parts of dam area to evaluate which arrangement could obtain better responses. For the former, both the transmitting and receiving electrodes remain on the survey line; while for the latter, there is a transmitting electrode placed far away. We use the same resistivity model for the inversion of the two sets of data. According to Figure 2, both sets of data reflect the high-resistance anomalies in the shallow and deep parts and low-resistance characteristics in the intermediate layer. However, for the dipole device, only the low-resistance anomaly in the first half of the survey line is resolved, and there is a false low-resistance anomaly about 10 meters below the 100-meter mark of the survey line. On the other hand, the pole-dipole configuration not only identifies the low-resistance anomaly in the second half of the survey line, but it also shows a continuous shape of the shallow high-resistance body. The pole-dipole array is hence chosen for subsequent electrode arrangement.

We hire two local fishing boats to lay the cable at the bottom of the water. One boat carries the resistivity meter and the cable with electrodes A, M, and N. Electrode B, connected to a 30 cm-long titanium plate is placed 1 kilometer downstream from the survey line. During the measurement, the main boat moves along the survey line, and the cable is manually laid into the water (Figure 3). To reduce the interference water flow may have on the position of the electrodes, we add the 1.5 kg-weight every 3-4 electrodes.

After we place the A, M, N electrodes in the water, the boat is anchored to fix them in the water, whilst the other boat drags the B electrode cable to its set location. The resistivity meter takes measurement according to the pre-set script, repeating three times for each measurement, taking about 30 minutes to collect 740 data points. The main boat moves along the survey line for subsequent measurements, with the starting point of the next cable placement as the midpoint of the previous placement. Every measurement shares an overlap with the last one to improve the observation accuracy through repetition of measurement. At the end, a total of 26,640 data points is collected. In operation, due to the complex terrain of the river channel and the shallow water where the boats could not pass, the electrodes must be laid manually by operators standing the river.

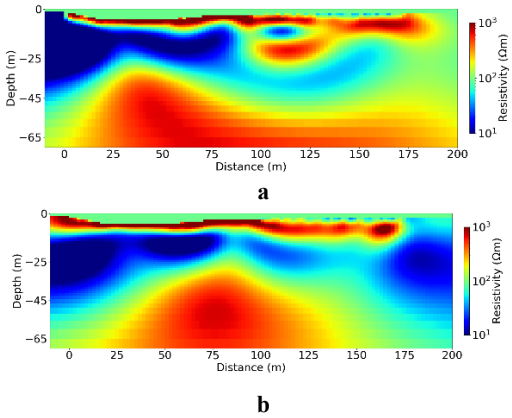


Figure 2: The initial resistivity model contains two layers. The upper layer is a fixed water layer with a resistivity of 100 ohm-m. The background resistivity is 200 ohm-m. **a** dipole-dipole configuration; **b** pole-dipole configuration.

Figure 3: The left figure shows the cable placing process by manpower in shallow water. The right figure shows the main boat that moves along the survey line until all the electrodes are laid on the river bottom.

## Results

To analyze the collected ERT data, we first check the quality of the measured potential difference and eliminate outliers.

The terrain of the riverbed is imported into the 2D inversion model, and the positions of the electrodes are placed at the interface between the water layer and the background rock layer. The resistivity of the water layer is 100 ohm-m, and the resistivity of the background model is 200 ohm-m. The resistivity inversion imaging is performed using the SimPEG inversion program. During the inversion, the water layer is fixed, and error misfit is controlled within 5%. The cross-sections of resistivity shown in Figure 4 and Figure 5 reveal that the region below the river water is mainly composed of three layers. The top layer is a high-resistance layer with good continuity and relatively uniform distribution. The borehole data infers sand, gravel, and pebbles deposited in the riverbed. The uneven particle size and poor sorting of the rock endow them a relatively high resistance which coincides with our inversion result. The resistivity below this layer changes dramatically in the lateral direction, showing overall low resistance. The second layer consists of rocks rich in pore water, which we interpret to be sandstone and weathered shale. The high-resistance body at the bottom made up the basement rock layer composed mainly of un-weathered limestone. Boreholes data shows that caves are mostly developed in limestone. Due to the high resistance shielding effect, the small scale of cave development, and deep burial, caves are not shown directly in the resistivity inversion section.

## Conclusions

This study demonstrates that the bold attempt to use the ERT method in rivers, mutually verified with existing borehole data and geological inferences can delineate the locations of potential caves and improve the understanding of regional geology. Like other geophysical methods, the ERT method has limitations and non-uniqueness of inversion results. To address this, we incorporate terrain and river water conductivity into the inversion model to reduce ambiguity. In terms of electrical structure, ERT effectively identifies rocks with high electrical conductivity, such as sandstone and shale, and delineates the spatial distribution of sand, gravel, and pebbles in the shallow region, as well as basement limestone, providing a reliable basis for finding potential karst caves.

## Acknowledgments

Here I would like to express my gratitude to my graduate student Yuan Zhao and residents Li Guangyao and Zhai Yemei for assisting in laying out the ERT survey lines.

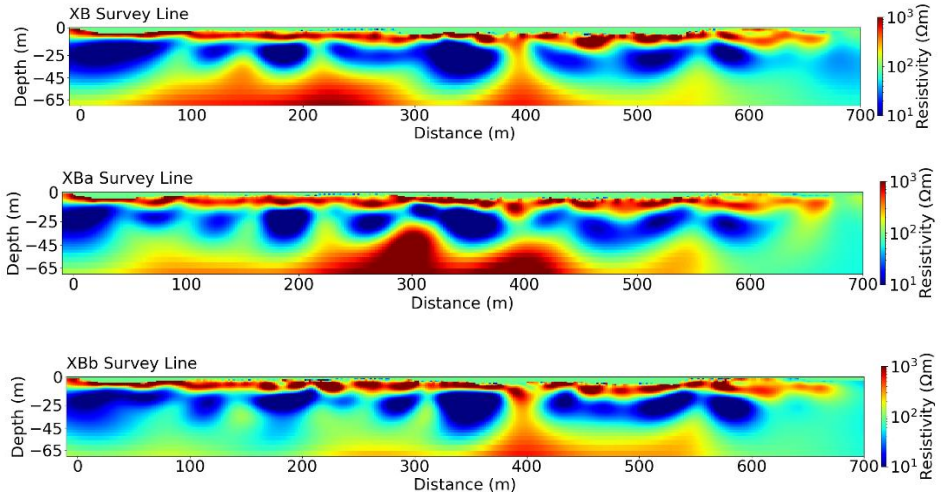


Figure 4: Three cross section of resistivity from data in the lower half of the dam. The shallow high-resistance anomalous bodies in each electrical profile are distributed continuously. The low-resistance bodies of the three survey lines develop continuously in space.

DOI:10.1190/iceg2023-032.1

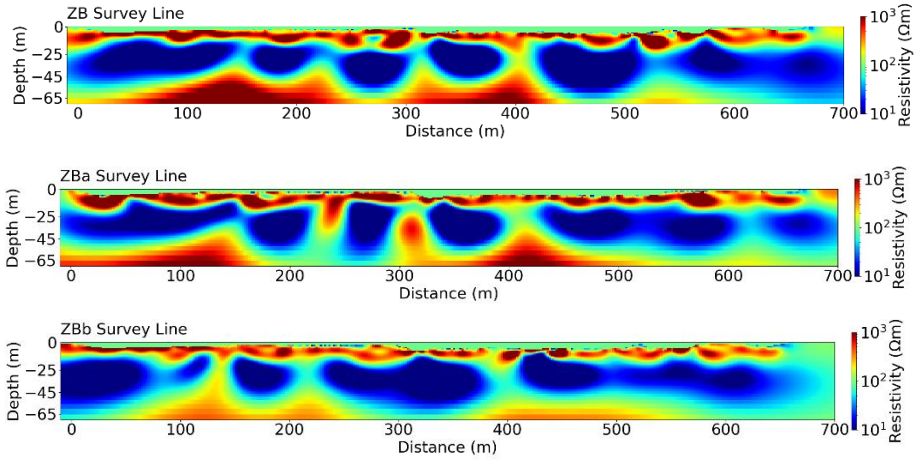


Figure 5: Three electrical profiles are in the middle of the dam area. Like Fig. 4, each electrical profile's shallow high-resistance anomalous bodies are distributed continuously. The bedrock appeared as high resistance in the profiles, and low-resistance bodies were continuous horizontally in the profiles.

**References**

[1] Wang, T. P. , Chen, Y. T. , Chen, C. C. , Tung, T. H. , & Yu, C. Y. . (2020). Application of cross-hole electrical resistivity tomography to groundwater contaminated remediation site. Terrestrial Atmospheric and Oceanic Sciences, 31(5), 507-521.

[2] Niculescu, B. M. , & Andrei, G. . (2021). Application of electrical resistivity tomography for imaging seawater intrusion in a coastal aquifer. Acta Geophysica(13).

[3] Tsokas, G. N. , Tsourlos, P. I. , Vargemezis, G. N. , & Pazaras, N. T. . (2011). Using surface and cross-hole resistivity tomography in an urban environment: an example of imaging the foundations of the ancient wall in thessaloniki, north greece. Physics & Chemistry of the Earth, 36(16), 1310-1317.

[4] Ping-Yu, C. , Chien-Chih, C. , Shu-Kai, C. , Tzu-Bin, W. , Chien-Ying, W. , & Shu-Kun, H. . (2012). An investigation into the debris flow induced by typhoon morakot in the siaolin area, southern taiwan, using the electrical resistivity imaging method. Geophysical Journal International(3), 1012-1024.

[5] Brunet, P. , R Clément, & Bouvier, C. . (2010). Monitoring soil water content and deficit using electrical resistivity tomography (ert) – a case study in the cevennes area, france. Journal of Hydrology, 380(1-2), 146-153.

[6] Cockett, R. , Kang, S. , Heagy, L. J. , Pidlisecky, A. , & Oldenburg, D. W. . (2015). Simpeg: an open source framework for simulation and gradient based parameter estimation in geophysical applications. Computers & Geosciences, 85(DEC.PT.A), 142-154.

[7] Okpoli, & Chibueze, C. . (2013). Sensitivity and resolution capacity of electrode configurations. International Journal of Geophysics, 2013, 1-12.

[8] Dale, F., Rucker, Danney, R., & Glaser. (2015). Standard, random and optimum array conversions from two-pole resistance data. Journal of Environmental & Engineering Geophysics, 20(3), 207-217.